03,16

Effect of Ge nanolayers and quantum dots on photoluminescence properties of GeSiSn/Si MQW heterostructures

© D.V. Kolyada[1], D.D. Firsov[1], O.S. Komkov[1], I.V. Skvortsov[2], V.I. Mashanov[2], I.D. Loshkarev[2], V.A. Timofeev[2]

[1] St. Petersburg State Electrotechnical University „LETI"
St. Petersburg, Russia
[2] Rzhanov Institute of Semiconductor Physics, Russian Academy of Sciences, Siberian Division, Novosibirsk, Russia

E-mail: kolyada.dima94@mail.ru, d.d.firsov@gmail.com

Received August 11, 2025
Revised September 2, 2025
Accepted September 7, 2025

Heterostructures with multiple GeSiSn/Si quantum wells including thin germanium layers, as well as with germanium quantum dots placed on top of the quantum wells, are studied. The heterostructures were grown by molecular beam epitaxy on silicon substrates. Structural studies using the X-ray diffraction method confirmed the elastically stressed state of the layers. Photoluminescence spectroscopy revealed that an increase in the germanium layer thickness leads to a red shift in the emission peak of multiple quantum wells, while the experimental values of the transition energies correlate well with theoretical calculations. The use of germanium quantum dots grown on top of GeSiSn/Si quantum wells enables a further long-wavelength shift of the emission. The obtained results demonstrate the efficiency of fine-tuning the energy spectrum of GeSiSn/Si heterostructures by varying the parameters of Ge layers, and open up prospects for the development of highly efficient infrared emitting devices.

Keywords: Multiple quantum wells, Fourier transform infrared spectroscopy, quantum dots, germanium nanolayers, molecular beam epitaxy, X-ray diffraction.

DOI: 10.61011/PSS.2025.09.62349.228-25

1. Introduction

Continuous development of a semiconductor industry requires creating new materials compatible with silicon technology in order to solve tasks of modern optoelectronics. IV group semiconductor compounds, in particular, GeSiSn solid solutions generate considerable interest due to their potential for integration of photon and electron devices on a single silicon platform [1,2]. Adjustability of a band gap and lattice parameters by varying a content of tin and silicon makes these materials suitable for a wide spectrum of applications, including creation of photodetector and light-emitting devices in the near- and mid-infrared ranges [3–7]. Adding tin into a Ge(Si) matrix makes it possible to effectively modify a band structure of the material. With certain compositions, GeSn and GeSiSn manifest direct-band-gap properties, thereby making them very promising for emissive devices [8,9]. For unstressed GeSn layers, a direct-band-gap structure is realized with the tin content exceeding 6.5%, whereas tensile stresses of 1.4% reduce this threshold to 5.4% [10]. These unique properties made it possible to create GeSn-based lasers that operate at the wavelengths of up to 2.7 μm [11,12]. Despite these successes, the high tin content in the GeSn alloys causes such difficulties as segregation and formation of defects, thereby negatively affecting the structural and optic properties of the materials [13–15]. These limitations resulted in investigating the GeSiSn solutions, which provide improved thermal stability and reduction of a defect density due to increased mixing entropy [16,17]. While in the bulk GeSiSn layers an increase of the Si fraction complicates production of the direct-band-gap compositions, thereby reducing probability of radiative recombination, heterostructures with GeSiSn/Si multiple quantum wells (MQW) become promising candidates for optoelectronic applications due to their capability of localizing charge carriers and enhancing radiative recombination. These structures demonstrate photoluminescence (PL) in the mid-IR range (1.55−3.3 μm) and at the same time the best radiative characteristics and reduction of the defect concentration are achieved due to post-growth thermal treatment [18–20]. Modern growth methods such as molecular beam epitaxy (MBE) allow manufacturing dislocation-free heterostructures with the GeSiSn MQWs on silicon substrates, significantly improving their optoelectronic properties [21]. Practical application of these heterostructures includes designing infrared sensors and emitters for the industry and dual-use technologies such as thermovision imaging and target detection [22,23]. Their compatibility with the silicon technology makes them ideal for integration into existing CMOS platforms (complementary metal−oxide−semiconductor), providing economically effective production of high-performance devices [12,24]. The next stage of developing of studies of such heterostructure is to create quantum dots QDs based on the GeSiSn solid solution. These structures allow for effective localization of the charge carriers, thereby increasing probability of

radiative recombination and improving photoluminescence characteristics (PL) [25,26]. The methods of MBE and chemical vapor deposition (CVD) make it possible to create high-density arrays of GeSn quantum dots with a low defect density, thereby making them suitable for application in emitters and photodetectors that operate in the mid-infrared range [27,28].

This study is dedicated to investigating the structural and optical properties of the GeSiSn/Si multiple quantum wells of a various composition and geometry, including those containing the Ge layers above the solid solution layer. Adding the Ge layers can allow suppressing tin diffusion and shifting the radiation spectrum into a long-wavelength range, which is an important step for subsequent creation of more complex heterostructures, such as Ge quantum dots formed on top of the GeSiSn/Si quantum wells. The quantum dots are added in order to further shift the wavelength into the more long-wavelength infrared range, which is important for extending the operating spectral range of new-generation devices. Optimization of growth parameters of these structures will open up new possibilities for designing the emitters and photodetectors based on GeSiSn/Si, which can be widely applied in the modern optoelectronic systems.

2. Experiment

The heterostructures including 10 periods of GeSiSn/Si or Ge/GeSiSn/Si quantum wells as well as with the Ge quantum dots on top of the GeSiSn/Si quantum wells were grown on the Si(100) substrates by low-temperature molecular beam epitaxy. Adding the Ge layer makes it possible to reduce tin segregation when a multilayer periodic structure is grown. An MBE growth chamber was equipped with an electron-beam evaporator for Si and effusion cells for Sn and Ge. The GeSiSn and Ge layers were deposited at the temperature of 150 °C. Si spacer interlayers were deposited in two stages: first 2 nm at 150 °C, then 5 nm at 500 °C. The deposition rates were: Ge — 0.128–0.222 Å/s, Si — 0.017–0.24 Å/s, Sn — 0.019–0.062 Å/s. In the sample containing the quantum dots, Ge was deposited at the temperature of 200 °C until the quantum dots appeared. During the growth, the surface morphology was controlled by reflection high-energy electron diffraction (RHEED). RHEED patterns exhibited strands corresponding to superstructures and reflections from the Ge quantum dots. The quality of the heterostructures, the stress state and the composition of the GeSiSn layers in the structures were studied by X-ray diffractometry. Rocking curves were measured using a two-crystal X-ray diffractometer DSO-1T with a Ge(004) monochromator in Cu $K_{\alpha 1}$ radiation.

The optic properties of the heterostructures with the GeSiSn/Si multiple quantum wells were studied by photoluminescence spectroscopy. A measurement setup based on the Fourier-transform infrared (FTIR) spectrometer Vertex 80 was used [29]. Luminescence of the structures was excited by a diode laser designed to operate at the wavelength of 405 nm, thereby providing effective absorption within epitaxial layers with the quantum wells. The PL signal was recorded using the InSb photodetector cooled by liquid nitrogen. In order to exclude background thermal radiation on the PL measurements, an output signal of the photodetector was supplied to a lock-in amplifier tuned to a frequency of modulation of exciting laser radiation.

3. Results and discussion

We have studied two series of the heterostructures with the $Ge_{0.84}Si_{0.076}Sn_{0.084}$/Si multiple quantum wells, which contain the Ge nanolayers of the various thickness above the quantum wells. Each series included structures without the Ge layers, with the Ge layer of the thickness of 0.25 and 0.5 nm. The samples of both the series were different only by the quantum well thickness, the quantum well thickness of the series 1 was 1 nm, while that of the series 2 – 0.5 nm. Figure 1 shows the rocking curve (004) for the S397 sample (Table).

A sequence of diffraction maximums is observed from SL–3 to SL+1. Presence of a sequence of satellites confirms an elastically-stressed state in the multilayer periodic structure.

Parameters of the studied samples

	Series 1			Series 2		
Sample number	S329	S397	S386	S335	S387	S337
Thickness of the $Ge_{0.84}Si_{0.076}Sn_{0.084}$ layer, nm	1	1	1	0.5	0.5	0.5
Thickness of the Ge layer, nm	–	0.25	0.5	–	0.25	0.5

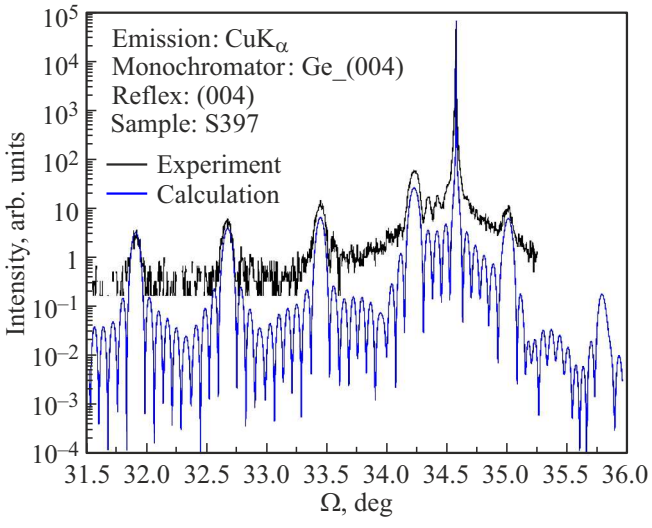

Figure 1. Experimentally obtained rocking curve (004) for the S397 structure as compared to modeling results.

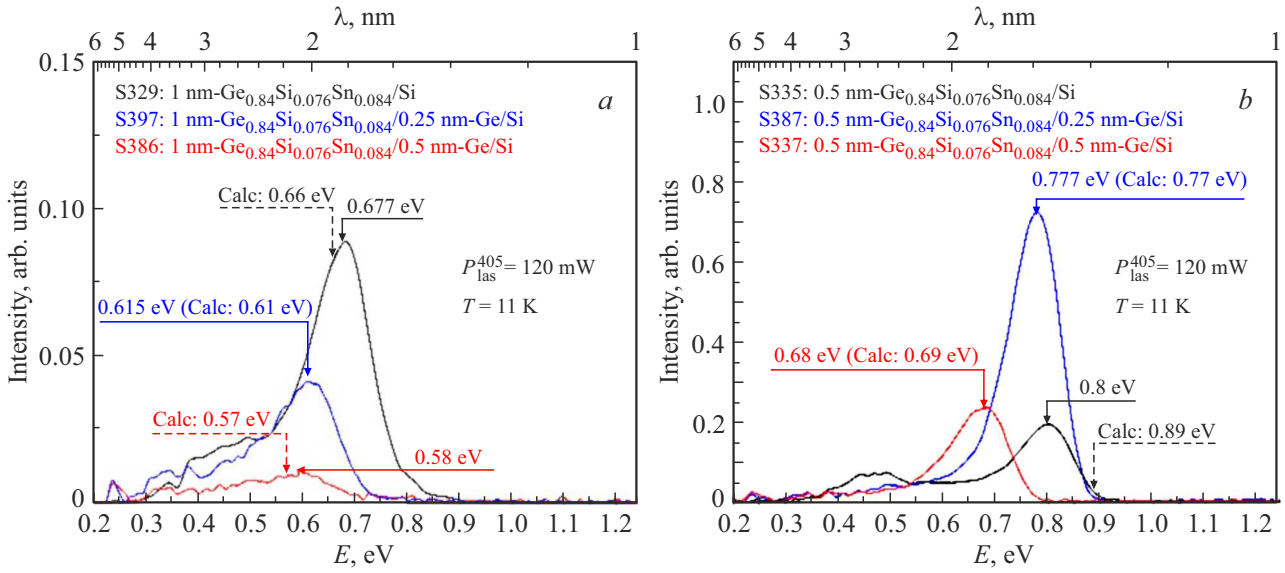

Figure 2. Photoluminescence of the structures that contain the $Ge_{0.84}Si_{0.076}Sn_{0.084}$/Si multiple quantum wells of the thickness of 1 nm (*a*) and the thickness of 0.5 nm (*b*). Intensity can be correctly compared only for the spectra shown in the same graph.

All the structures were subjected to high-temperature annealing within the temperature interval of 550–650 °C for 10 min in an argon atmosphere, thereby allowing significantly reducing a contribution by the structure defects into the luminescence [19]. As shown previously, the main defects in the structures of this type are vacancy-tin complexes [20].

Spectra of photoluminescence of the series 1 samples are shown in Figure 2, *a*, while those of the series 2 samples are shown in Figure 2, *b*. The observed PL peaks correspond to transitions from a Si Δ-valley into a level of dimensional quantization of heavy holes in the Ge/$Ge_{0.84}Si_{0.076}Sn_{0.084}$/Si quantum wells as shown in an energy band diagram (Figure 3). The energy band diagram was calculated by a method described in the study [30].

For the series 1 structure that does not contain the Ge layers, a position of the PL peak corresponds to the energy of 0.677 eV, which matches well with the calculated value (0.66 eV). For the structure with the Ge layer of the thickness of 0.25 nm, the PL peak is observed at the energy of 0.615 eV (the calculated value is 0.61 eV), while in case of the structure with the Ge layer's thickness of 0.5 nm it is observed at 0.58 eV (the calculated value is 0.57 eV). One can distinctly observe a tendency to PL shifting towards the long-wavelength values as the thickness of the Ge layers increases, wherein excellent consistency of the experimental and theoretical values is observed for the first series.

For the second series of the samples, which contains thinner (0.5 nm of GeSiSn) quantum wells, a similar tendency is observed — the position of the PL peak is shifted into the long-wavelength range when the thickness of the Ge layers increases. For the structure that does not contain the Ge layers, the position of the PL peak corresponds to the energy of 0.8 eV (the calculated value is 0.89 eV). For the structure with the Ge layer of the thickness of 0.25 nm, the PL peak is observed at the energy of 0.777 eV (the calculated value is 0.7 eV), while in case of the Ge layer's thickness of 0.5 nm it is observed at 0.68 eV (the calculated value is 0.69 eV). For the structures with the smaller thickness of the quantum wells, consistency of the experiment with the theoretical calculations turned out to be worse than for the wider quantum wells, which can be explained by the fact that in the narrower quantum wells tin diffusion is more pronounced due to high-temperature annealing.

Thus, based on the spectra of the structures, which are shown in Figure 2, it can be concluded that adding

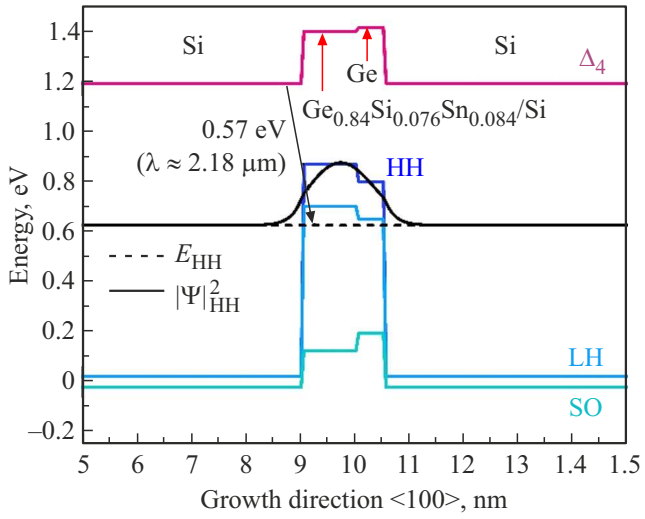

Figure 3. Energy band diagram of the S386 sample that contains the $Ge_{0.84}Si_{0.076}Sn_{0.084}$/Si multiple quantum wells of the thickness of 1 nm with the Ge layer of the thickness of 0.5 nm.

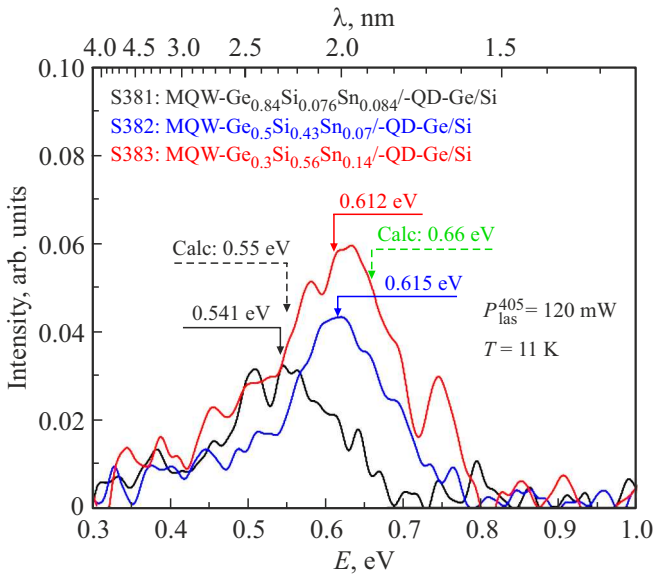

Figure 4. PL of structures containing Ge quantum dots on top of GeSiSn/Si quantum wells. Calculated values of the transitions in QWs for structures S382 and S383 are indicated in green.

the Ge layer on top of the GeSiSn/Si multiple quantum wells allows shifting radiation from the structures into the more long-wavelength spectral range. However, at the same time intensity of luminescence of the sample with the GeSiSn layer of the thickness of 1 nm is reduced, which can be induced by reduction of an overlap integral of wave functions of electrons in Si and holes in the wider Ge/GeSiSn/Si quantum wells. In order to reduce the influence of this drawback, we have grown the following series of the structures that contained the Ge quantum dots instead of the Ge nanolayers on top of the GeSiSn/Si quantum wells (Figure 4). The structures in this series were different only by the compositions of the quantum wells, the thickness of the quantum wells was 1 nm.

For the S381 structure the quantum wells' composition is $Ge_{0.84}Si_{0.076}Sn_{0.084}$, for the S382 structure the QW composition is $Ge_{0.5}Si_{0.43}Sn_{0.07}$ and for the S383 structure the QW composition is $Ge_{0.3}Si_{0.56}Sn_{0.14}$. The position of the PL peaks of these structures was determined by approximation by Gauss curves. All the structures exhibit good compliance of the experimental and calculated positions of energy transitions. For the S381 structure, the experimental value of E_g was 0.541 eV (the calculated value is 0.55 eV), for the S382 structure, $E_g = 0.615$ eV (the calculated value is 0.66 eV) and for the S383 structure, $E_g = 0.612$ eV (the calculated value is 0.66 eV). Thus, it is clear that the qualitative behavior of the structures quite well corresponds to the theoretical predictions. At the same time, we managed to achieve the even more significant shift of luminescence into the long-wavelength range as compared to the first-series structures and the highest wavelength of the PL peak was 2.29 μm.

4. Conclusion

During the performed studies, we have produced the complex structures including germanium nanolayers as well as the structures containing germanium quantum dots arranged on top of the GeSiSn multiple quantum wells, which can emit in a broad spectral range. The obtained experimental data demonstrate that adding the thin Ge layer to the structures with the GeSiSn/Si multiple quantum wells results in shifting of the photoluminescence peak into the long-wavelength spectral range. The measured PL spectra for the samples with the different thickness of the Ge layer well correlate with the theoretical calculations, thereby confirming that it is possible to finely tune the band structure by varying the thickness of the added layers. However, the narrower quantum wells turned out to be more sensitive to the effects of tin diffusion, which results in some discrepancies between the experimental values and the calculated data. The observed tendency to shifting of the energy transitions indicates the effective influence of additional Ge components on the parameters of the quantum wells, which is a significant factor for designing silicon-based optoelectronic devices. Further improvement of process parameters, including control of the layer thickness, adjustment of the tin diffusion processes and optimization of thermal treatment procedures, will allow increasing the radiation efficiency.

Funding

The study was performed within the framework of the state assignment of the Ministry of Education and Science of the Russian Federation for the Rzhanov Institute of Semiconductor Physics of the Siberian Branch of the Russian Academy of Sciences No. FWGW-2024-0001 „Physical and technological foundations of creating heterostructures based on group IV elements compatible with the modern silicon technology for photonics devices".

Conflict of interest

The authors declare that they have no conflict of interest

References

[1] G. Daligou, R. Soref, Anis Attiaoui, Md.J. Hossain, M.R.M. Atalla, P.D. Vecchio, O. Moutanabbir. IEEE JPV **13**, *5*, 728 (2023).
[2] C. Xu, L. Jiang, J. Kouvetakis, J. Menendez. Appl. Phys. Lett. **103**, *7*, 072111 (2013).
[3] G. Sun, R. Soref, J. Khurgin, S. Yu, G. Chang. Technical Digest Series (Optica Publishing Group) JW2A119 (2023).
[4] M.R.M. Atalla, S. Assali, G. Daligou, A. Attiaoui, S. Koelling, P. Daoust, O. Moutanabbir. ACS Photonics **11**, *3*, 1335 (2024).
[5] K.L. Low, Y. Yang, G. Han, W. Fan, Y.-C. Yeo. J. Appl. Phys. **112**, *10*, 103715 (2012).

[6] M. Oehme, M. Schmid, M. Kaschel, M. Gollhofer, D. Widmann, E. Kasper, J. Schulze. Appl. Phys. Lett. **101**, *14*, 141110 (2012).
[7] S. Gupta, B. Magyari-Kope, Y. Nishi, K.C. Saraswat. J. Appl. Phys. **113**, *7*, 073707 (2013).
[8] T.R. Harris, M.Y. Ryu, Y.K. Yeo, B. Wang, C.L. Senaratne, J. Kouvetakis. J. Appl. Phys. **120**, *8*, 085706 (2016).
[9] S. Wirths, R. Geiger, N. von den Driesch, G. Mussler, T. Stoica, S. Mantl, Z. Ikonic, M. Luysberg, S. Chiussi, J.M. Hartmann, H. Sigg, J. Faist, D. Buca, D. Grützmacher, Nature Photonics **9**, 88 (2015).
[10] A. Elbaz, D. Buca, N. von den Driesch, K. Pantzas, G. Patriarche, N. Zerounian, E. Herth, X. Checoury, S. Sauvage, I. Sagnes, A. Foti, R. Ossikovski, J.-M. Hartmann, F. Boeuf, Z. Ikonic, P. Boucaud, D. Grützmacher, M. El Kurdi. Nat. Photonics **14**, 375 (2020).
[11] Y. Zhou, S. Ojo, C.-W. Wu, Y. Miao, H. Tran, J.M. Grant, G. Abernathy, S. Amoah, J. Bass, G. Salamo, W. Du, G.-En Chang, J. Liu, J. Margetis, J. Tolle, Y.-H. Zhang, G. Sun, R.A. Soref, B. Li, S.-Q. Yu. Photon. Res. **10**, *1*, 222 (2022).
[12] Y. Zhou, Y. Miao, S. Ojo, H. Tran, G. Abernathy, J.M. Grant, S. Amoah, G. Salamo, W. Du, J. Liu, J. Margetis, J. Tolle, Y. Zhang, G. Sun, R.A. Soref, B. Li, S.-Q. Yu. Optica **7**, *8*, 924 (2020).
[13] J. Nicolas, S. Assali, S. Mukherjee, A. Lotnyk, O. Moutanabbir. Cryst. Growth Des. **20**, *5*, 3493 (2020).
[14] P.R. Pukite, A. Harwit, S.S. Iyer. Appl. Phys. Lett. **54**, *21*, 2142 (1989).
[15] J. Xie, A.V.G. Chizmeshya, J. Tolle, V.R. D'Costa, J. Menendez, J. Kouvetakis. Chemistry of Materials **22**, 3779 (2010).
[16] V. Timofeev, A. Nikiforov, A. Tuktamyshev, V. Mashanov, M. Yesin, A. Bloshkin. Nanoscale Res. Lett. **13**, 29 (2018).
[17] S. Assali, J. Nicolas, O. Moutanabbir. J. Appl. Phys. **125**, *2*, 025304 (2019).
[18] V. Timofeev, V.I. Mashanov, A.I. Nikiforov, I.D. Loshkarev, I.V. Skvortsov, D.V. Gulyaev, I.V. Korolkov, D.V. Kolyada, D.D. Firsov, O.S. Komkov. Rus. Phys. J. **64**, 1505 (2021).
[19] D.V. Kolyada, D.D. Firsov, V.A. Timofeev, V.I. Mashanov, A.A. Karaborchev, O.S. Komkov. Semiconductors **56**, *8*, 547 (2022).
[20] V. Timofeev, I. Skvortsov, V. Mashanov, A. Nikiforov, D. Kolyada, D. Firsov, O. Komkov, S. Samadov, A. Sidorin, O. Orlov. J. Vac. Sci. Technol. B **42**, *8*, 030601 (2024).
[21] N. von den Driesch, D. Stange, D. Rainko, I. Povstugar, P. Zaumseil, G. Capellini, T. Schröder, T. Denneulin, Z. Ikonic, J.-M. Hartmann, H. Sigg, S. Mantl, D. Grützmacher, D. Buca. Adv. Sci. **5**, *6*, 1700955 (2018).
[22] R. Soref. Nature Photonics **4**, 495 (2010).
[23] G. Sun, R.A. Soref, H.H. Cheng. Opt. Express **18**, *19*, 19957 (2010).
[24] V.A. Timofeev, V.I. Mashanov, A.I. Nikiforov, I.V. Skvortsov, A.E. Gayduk, A.A. Bloshkin, I.D. Loshkarev, V.V. Kirienko, D.V. Kolyada, D.D. Firsov, O.S. Komkov. Appl. Surf. Sci. **593**, 153421 (2022).
[25] R. Bar, A.K. Katiyar, R. Aluguri, S.K. Ray. Nanotechnology **28**, *29*, 2095201 (2017).
[26] V. Schlykow P. Zaumseil, M.A. Schubert, O. Skibitzki, Y. Yamamoto, W.M. Klesse, Y. Hou, M. Virgilio, M. De Seta, L. Di Gaspare, T. Schroeder, G. Capellini. Nanotechnology **29**, *41*, 415702 (2018)
[27] F. Oliveira, I.A. Fischer, A. Benedetti, M.F. Cerqueira, M.I. Vasilevskiy, S. Stefanov, S. Chiussi, J. Schulze. J. Appl. Phys. **117**, *12*, 125706 (2015).
[28] V. Timofeev, I. Skvortsov, V. Mashanov, A. Nikiforov, I. Loshkarev, A. Bloshkin, V. Kirienko, D. Kolyada, D. Firsov, O. Komkov. IEEE Journal of Selected Topics in Quantum Electronics **31**, *1*, 8200108 (2025).
[29] D.D. Firsov, O.S. Komkov, V.A. Solov'ev, P.S. Kop'ev, S.V. Ivanov. J. Phys. D: Appl. Phys. **49**, *28*, 285108 (2016).
[30] V.A. Timofeev, I.V. Skvortsov, V.I. Mashanov, A.E. Gayduk, A.A. Bloshkin, V.V. Kirienko, D.E. Utkin, A.I. Nikiforov, D.V. Kolyada, D.D. Firsov, O.S. Komkov. Appl. Surf. Sci. **659**, 159852 (2024).

Translated by M.Shevelev